Adsorption on Inkjet-Printable Polyelectrolyte Hydrogels Allows Refractive Index Sensing of Diclofenac and Metoprolol in Aqueous Solution

Alexander Southan,* Jennifer Tan, Fabian Schuster, Julia Rotenberger, and Günter E. M. Tovar

Read Online

ACCESS | Metrics & More | Article Recommendations | Supporting Information

ABSTRACT: Polyelectrolyte hydrogels containing negatively charged sulfonate groups or positively charged ammonium groups are characterized by their adsorption behavior toward the pharmaceuticals metoprolol (cationic) and diclofenac (anionic) in an aqueous solution. Additionally, the change in the hydrogel refractive index with metoprolol and diclofenac concentrations inside the hydrogel is investigated. Both metoprolol adsorption on sulfonate group containing hydrogels as well as diclofenac adsorption on the ammonium group containing hydrogels can be described using a modified Langmuir-type adsorption isotherm with K_s values around 0.1 and 10 mL μmol^{-1}, respectively. In both cases, the adsorption capacities are close to the concentration of charged groups in the hydrogels. Thus, diclofenac concentrations inside the hydrogels are enhanced by a factor of approximately 1000 and metoprolol concentrations by a factor of approximately 10 compared to their concentrations in solution. In contrast, metoprolol was completely excluded from the ammonium group containing hydrogels, and diclofenac showed weak adsorption on the poly(ethylene glycol) fraction of the sulfonate group containing hydrogels, resulting in lower concentration enhancements. Hydrogel refractive indices increased linearly with the concentration of metoprolol and diclofenac inside the hydrogels. Thus, monitoring the refractive index of sulfonate group containing hydrogels is shown to be efficient in measuring the solution concentrations of metoprolol up to 10 μmol mL^{-1} and of ammonium group containing hydrogels for diclofenac concentrations up to 0.1 μmol mL^{-1}, both values corresponding to the reciprocal of the K_s values. In the case of Langmuir-type adsorption, maximizing K_s values therefore leads to the best refractive index sensor sensitivities at low analyte concentrations, whereas lower K_s values lead to lower sensitivities at low concentrations but to superior sensitivities at rather high analyte concentrations. Inkjet printing of the hydrogel formulations is demonstrated to facilitate their future use as spatially resolved coatings on sensor surfaces.

KEYWORDS: Langmuir, adsorption, isotherm, partition, ion exchange, HPLC, Donnan exclusion
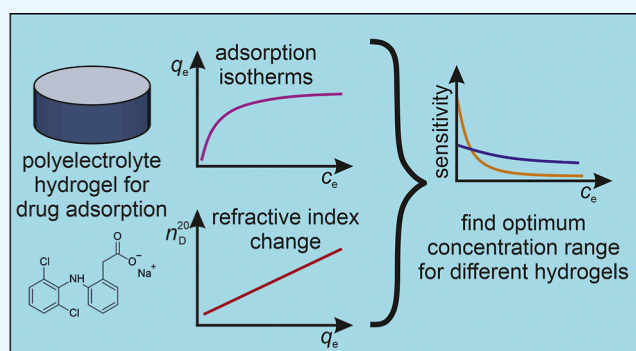
INTRODUCTION

Hydrogels consist of cross-linked polymer networks swollen by an aqueous medium throughout their volume[1] and are applied for various purposes, including drug delivery,[2,3] tissue engineering,[4] or sensing in aqueous environments.[5,6] One key feature of hydrogels is that they are permeable for water and other small molecules by diffusion so that they can distribute within the entire volume of the hydrogel.[7,8] Therefore, when placing a hydrogel into a solution of an analyte of interest, interactions between the analyte and all of the components present in the hydrogel can occur, changing the chemical composition of the combination of polymer network and swelling medium. The extent of the alteration of hydrogel composition depends on the type and strength of the interactions, and thus, e.g., on the presence of functional groups in the polymer network or the analyte. For example, Singha et al. showed that adsorption of Co(II), Cu(II), Zn(II),

and Pb(II) ions on hydrogels containing carboxy groups can be described with a Langmuir adsorption isotherm,[9] presumably due to an ion exchange mechanism. Fei et al. studied the adsorption of the antibiotic ciprofloxacin on alginate hydrogels containing graphene oxide (GO) and found that the addition of GO increased the adsorption capacity compared to pure alginate hydrogels.[10] Also, their adsorption isotherms were fitted with a Langmuir model. These examples demonstrate
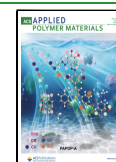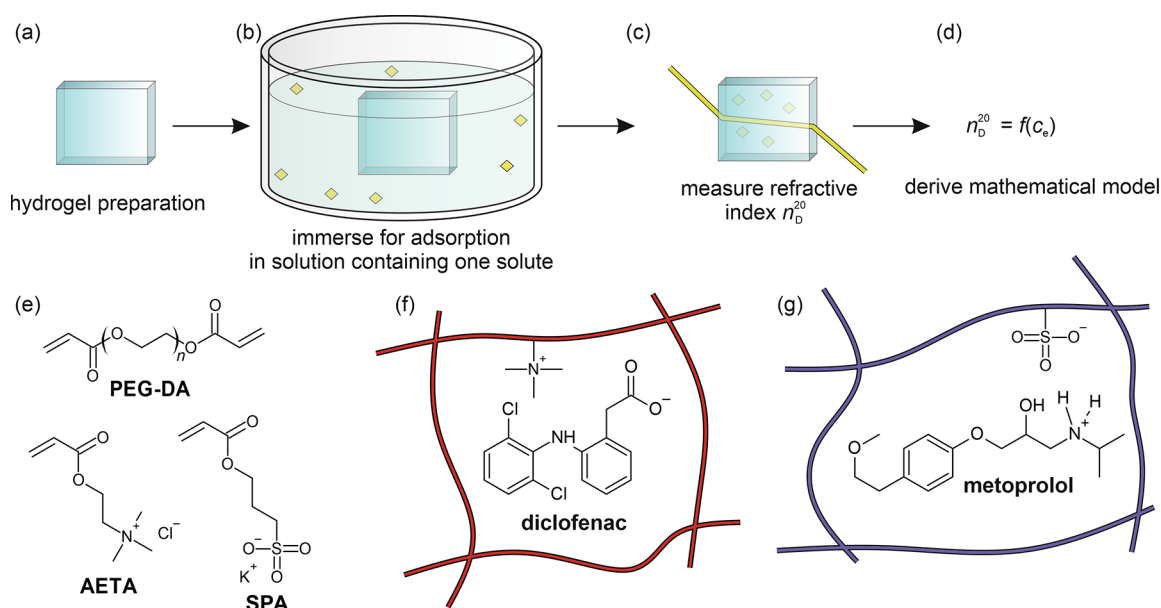
Figure 1. Schematic representation of the concept applied in this study to use polyelectrolyte hydrogels as sensors for ionic solutes. (a) First, polyelectrolyte hydrogels containing either quaternary ammonium or sulfonate groups are prepared by photochemical cross-linking. (b) For adsorption of a solute, a hydrogel is immersed in a solution containing either diclofenac or metoprolol. (c) Refractive index n_D^{20} of the hydrogel is measured after adsorption, and (d) collected data are used to fit a mathematical model describing the sensor response as a function of solute concentration c_e. (e) Chemical structures of hydrogel building blocks poly(ethylene glycol)diacrylate (PEG-DA), sulfopropyl acrylate potassium salt (SPA), and [2-(acryloyloxy)ethyl]trimethylammonium chloride (AETA). (f) Interaction of diclofenac with the quaternary ammonium groups inside the hydrogels and (g) interaction of metoprolol with the sulfonate groups.

that the change in hydrogel composition with analyte concentration is often nonlinear.

The change in hydrogel composition upon adsorption of analytes induces a change in hydrogel properties, e.g., in electrochemical properties[11,12] or optical properties such as the refractive index.[13] Therefore, reading hydrogel properties in the presence of an analyte with appropriate transducers can be used for sensing the analyte concentration. A broad spectrum of optical readout methods relies on measuring the refractive index in close proximity to the transducer. Examples are surface plasmon resonance spectroscopy (SPRS),[14−16] reflectometric interference spectroscopy,[17] or approaches based on interferometers such as Mach−Zehnder interferometers or dual-mode interferometers.[18,19] One big advantage of the combination of such a method sensitive to refractive index changes with a material such as a hydrogel is that due to analyte adsorption on the hydrogel, the concentration of the analyte near the transducer surface can be enhanced greatly by adsorption, and thus, the sensor sensitivity is also enhanced.

However, the prediction of the sensor response of a specific hydrogel in combination with a given transducer is challenging. As explained above, hydrogels as functional adsorbers on transducers usually result in a nonlinear response of the optical properties of the hydrogel with the analyte concentration. This nonlinear response is a result of strong or weak interactions between the polymer network, the swelling medium, and the analyte, diffusion of the analyte into and out of the aqueous swelling medium, and other effects such as size exclusion or Donnan exclusion.[20] Therefore, in order to optimize the interaction of hydrogels with a given analyte, the chemical composition of a functional hydrogel has to be tailored according to the chemical composition of the analyte, and the adsorption behavior needs to be characterized in detail, which is often omitted.[12,17,21]

Important analytes in aqueous solutions are impurities that can be found in surface water, especially pharmaceuticals such as diclofenac and metoprolol.[22] In aqueous solutions, these two compounds are usually are present in their ionic forms, e.g., diclofenac sodium salt and metoprolol tartrate. Therefore, we hypothesize that polyelectrolyte hydrogels with permanently charged functional groups are efficient adsorbers for such compounds, leading to a large enhancement of diclofenac and metoprolol concentrations inside the hydrogels. In this study, we aim to characterize the adsorption behavior of diclofenac and metoprolol on polyelectrolyte hydrogels containing either quaternary ammonium groups or sulfonate groups (Figure 1). Additionally, we demonstrate that the hypothesized concentration enhancement leads to an enhancement in the change in refractive index, which will make such hydrogels interesting for functional coatings on sensor surfaces. We aim to describe the hydrogel adsorption and refractive index behavior with mathematical models in order to predict their response to certain diclofenac and metoprolol concentrations. Finally, the processing of such hydrogels to coatings by inkjet printing will be investigated, which may lead to sensor coatings with spatial resolution in future studies.

■ EXPERIMENTAL SECTION

Materials. Poly(ethylene glycol) diacrylate (PEG-DA, M_n = 700 g mol^{-1}), 3-sulfopropyl acrylate potassium salt (SPA), [2-(acryloyloxy)-ethyl]trimethylammonium chloride (AETA, 80 wt % in H$_2$O), Irgacure 2959, 2-(N-morpholino)ethanesulfonic acid sodium salt (MES sodium salt), diclofenac sodium salt, and (±)-metoprolol (+)-tartrate salt were obtained from Sigma-Aldrich. Acetonitrile for HPLC was obtained from Honeywell. 2-(N-Morpholino)-ethanesulfonic acid (MES) was obtained from Carl Roth GmbH (Germany). Water was withdrawn from a Barnstead GenPure xCAD water purification system (Thermo Scientific). MES buffer (20 mM, pH

6.0) for HPLC was obtained by dissolving 10 mmol MES and 10 mmol MES sodium salt in 1 L of water.

Hydrogel Preparation and Characterization. Stock solutions with a concentration of 7 mg/g (w/w) of the photoinitiator Irgacure 2959 were prepared by mixing 35.0 mg of Irgacure 2959 with 4.965 g of water. The mixture was heated with a heat gun to approximately 100 °C and shaken until all Irgacure 2959 was dissolved. Hydrogel precursor solutions were prepared by mixing appropriate amounts of PEG-DA, a monomer with an ionic group (either AETA or SPA), Irgacure 2959 stock solution, and water. SPA and AETA concentrations were 1, 3, and 5% (w/w), respectively, and corresponding PEG-DA concentrations were 19, 17, and 15%, respectively, so that the total concentration of polymerizable compounds amounted to 20% (w/w). As a reference, hydrogels containing no ionic monomer but 20% (w/w) PEG-DA were prepared. The Irgacure 2959 concentration was 0.1% (w/w) in all cases. Samples were named according to their AETA and SPA concentrations, making the samples SPA5 and AETA5 hydrogels with 5% (w/w) SPA and AETA in the hydrogel precursor solution, respectively. In a typical example of an SPA5 hydrogel, 50 mg of SPA were mixed with 150 mg of PEG-DA and 143 mg of Irgacure 2959 stock solution, containing 1 mg of Irgacure 2959, were added, followed by 657 mg of water. The mixture was shaken, until a clear solution was obtained. For curing, 750 μL of a hydrogel precursor solution was pipetted into a cylindrical aluminum mold with a diameter of 3 cm and a depth of 1 mm, covered with a quartz glass pane, and irradiated in a UV chamber (Sol2, Dr. Hönle AG, Germany) at an intensity of 50 mW cm^{-2} for 7.5 min. After that, the hydrogels were removed from the molds with a spatula and weighed for mass m_0 directly after preparation. The hydrogels were then washed and swollen to equilibrium with water for 72 h, exchanging water every 24 h. Subsequently, the hydrogels were blotted dry with filter paper and were either used for adsorption experiments (see description below) or characterized further for the equilibrium degree of swelling (EDS) and gel yield (Y). For the latter purpose, the hydrogels were weighed for the mass m_s of the swollen hydrogels and then dried at a pressure of 30 mbar and a temperature of 60 °C in a vacuum oven until a constant mass was obtained (typically 24 h). The hydrogels were then weighed for the mass m_d of the dried hydrogel. From the resulting values, EDS and Y were calculated as follows

$$EDS = \frac{m_s}{m_d} \tag{1}$$

$$Y = \frac{m_d}{m_0 \cdot 0.2} \tag{2}$$

The water volume fraction ϕ_{H_2O} inside the hydrogels was calculated assuming that mass and volume fractions were identical (density of the hydrogel $\rho_H = 1$ g mL^{-1}) as

$$\phi_{H_2O} = 1 - EDS^{-1} \tag{3}$$

In order to calculate the concentrations of c_{sulfo} and c_{ammon} of sulfonate groups from SPA and quaternary ammonium groups from AETA, respectively, in the hydrogels after swelling to equilibrium, it was assumed that PEG-DA and the ionic monomers are present in the gel fraction with the same composition as in the hydrogel precursor solutions. Calculations were done with the following equations

$$c_{sulfo} = \frac{w_{SPA}}{(w_{PEG-DA} + w_{SPA}) \cdot M_{SPA} \cdot EDS} \tag{4}$$

$$c_{ammon} = \frac{w_{AETA}}{(w_{PEG-DA} + w_{AETA}) \cdot M_{AETA} \cdot EDS} \tag{5}$$

Here, w_{PEG-DA}, w_{SPA}, and w_{AETA} are the mass fractions of PEG-DA, SPA, and AETA, respectively, in the hydrogel precursor solutions, and M_{SPA} and M_{AETA} are the corresponding molar masses (232.30 g mol^{-1} for SPA and 193.67 g mol^{-1} for AETA).

Adsorption Experiments. All adsorption experiments were carried out with hydrogels directly after swelling to equilibrium at

20 °C. For this purpose, hydrogels were cut into pieces, and their masses m_H were determined accurately. These hydrogel pieces were immersed into a volume $V_0 = 1$ mL of either diclofenac or metoprolol. Concentrations c_0 of both diclofenac and metoprolol before adsorption were 1 mg mL^{-1} for AETA hydrogels and 10 mg mL^{-1} for SPA hydrogels. The mixtures were shaken gently on an orbital platform shaker (200 rpm) for a defined time for the determination of adsorption kinetics and for 24 h for the adsorption isotherms. The supernatant was transferred into HPLC vials, and resulting diclofenac and metoprolol concentrations c_e were determined by HPLC. The ratio a_e of the amount of diclofenac or metoprolol present per mass of hydrogel was calculated as

$$a_e = \frac{(c_0 - c_e) \cdot V_0}{M_{ads} \cdot m_H} \tag{6}$$

M_{ads} is the molar mass of the adsorbed compounds, which are 684.81 g mol^{-1} for metoprolol tartrate (containing 2 mol of metoprolol cations per mole) and 318.13 g mol^{-1} for diclofenac sodium salt. Thus, experimental a_e values were calculated from the known values of c_0, V_0, M_{ads}, and m_H together with the measured value of c_e. Note that all concentrations for metoprolol in this study were calculated with the mentioned molar mass, so they would have to be multiplied by a stoichiometric factor of 2 when the concentration of metoprolol cations is relevant.

From the experimental a_e values, the partition coefficients k, defined as the ratio of average adsorbate concentration $c_{e,H}$ in the hydrogel and c_e, the surrounding solution equilibrium concentration, were calculated. The partition coefficient k is given with the hydrogel density ρ_H as

$$k = \frac{c_{e,H}}{c_e} = \frac{a_e \cdot \rho_H}{c_e} \tag{7}$$

Under ideal partition conditions without the presence of interactions between the polymer network and the adsorbates, k equals the water volume fraction $\phi_{H_2O} = V_{H_2O}/V_{gel}$ as the ratio of water volume V_{H_2O} inside the hydrogel and the total hydrogel volume V_{gel}.[23] Therefore, an enhancement factor E describing the ratio of real and ideal partition coefficients was calculated by[20]

$$E = \frac{k}{\phi_{H_2O}} \tag{8}$$

Model for Adsorption on Hydrogels. For analyzing the adsorption experiments, we generally followed the reasoning of Gulsen and Chauhan.[24] Thus, a_e is regarded as a result from contributions of adsorbate present in the aqueous phase inside the hydrogel with a concentration $c_{e,H,aq}$ and of adsorbate adsorbed on the polymer network. The amount of adsorbate adsorbed on the polymer network per mass of the hydrogel can, in some cases, be described with a Langmuir model with q_m (adsorption capacity) and K_s (ratio of adsorption and desorption rate constants)

$$q_e = q_m \cdot \frac{K_s \cdot c_{e,H,aq}}{1 + K_s \cdot c_{e,H,aq}} \tag{9}$$

In the Langmuir adsorption case, with the water volume fraction $\phi_{H_2O} = V_{H_2O}/V_{gel}$, a_e becomes

$$a_e = \frac{c_{e,H,aq} \cdot \phi_{H_2O}}{\rho_H} + q_e = \frac{c_{e,H,aq} \cdot \phi_{H_2O}}{\rho_H} + q_m \cdot \frac{K_s \cdot c_{e,H,aq}}{1 + K_s \cdot c_{e,H,aq}} \tag{10}$$

As can be seen from eq 10, the interaction of the adsorbate solutions with the hydrogels results from a partition term and a Langmuir adsorption term, which both depend on $c_{e,H,aq}$. It was assumed that $c_{e,H,aq}$ is isotropic throughout the aqueous phase inside the hydrogel in order to be able to treat the two contributions independently of each other.

In some cases, q_e was best described with an empirical polynomial model

$$q_e = b_1 \cdot c_{e,H,aq}^3 + b_2 \cdot c_{e,H,aq} \tag{11}$$

In this case, a_e becomes

$$a_e = \frac{c_{e,H,aq} \cdot \phi_{H_2O}}{\rho_H} + b_1 \cdot c_{e,H,aq}^3 + b_2 \cdot c_{e,H,aq} \tag{12}$$

Combining eqs 7, 8 and 10, an expression for the enhancement factor in the Langmuir adsorption case is obtained

$$E = \frac{c_{e,H,aq}}{c_e} \cdot \left(\frac{\rho_H}{\phi_{H_2O}} \cdot q_m \cdot \frac{K_s}{1 + K_s \cdot c_{e,H,aq}} + 1 \right) \tag{13}$$

Similarly, by combining eqs 7, 8 and 12, an expression for the enhancement factor in the polynomial adsorption case is obtained

$$E = \frac{c_{e,H,aq}}{c_e} \cdot \left[\frac{\rho_H}{\phi_{H_2O}} \cdot (b_1 \cdot c_{e,H,aq}^2 + b_2) + 1 \right] \tag{14}$$

HPLC Measurements. HPLC measurements were performed on a Shimadzu HPLC system with an isocratic flow (1 mL min^{-1}) of 20% acetonitrile and 80% MES buffer at a temperature of 40 °C and with an injection volume of 10 μL. The column used for separation was a Vydac 214TP C4 5 μ (Grace). Elugrams of diclofenac and metoprolol were evaluated measuring UV absorption at 280 and 276 nm, respectively. Calibrations for metoprolol and diclofenac concentration measurements were carried out with six individually prepared standard solutions in water for each compound with concentrations of approximately 0.2, 0.4, 0.6, 0.8, 1.0, and 1.2 mg mL^{-1} and subsequent linear regression of the integrals. 100 μL of the SPA hydrogel supernatants were diluted with 900 μL water prior to measurements, whereas AETA hydrogel supernatants were measured directly. For quantification purposes, elugrams were integrated between elution volumes of 6.5 and 12.5 min for metoprolol and between 12.5 and 18.5 min for diclofenac.

Refractive Index Measurements. Hydrogel refractive indexes n_D^{20} were measured using a digital refractometer DR301−95 (Krüss, Germany). For this purpose, hydrogel discs with a diameter of 7 mm were punched out of the hydrogels and pressed on the measurement window by a metal spring, which was placed between the lid and the sample. The temperature for all measurements was 20 °C.

Characterization of Hydrogel Formulations for Inkjet Printing. Inkjet inks have to meet certain criteria to be jettable from an inkjet printhead.[25,26] Therefore, the hydrogel formulations were characterized by means of density ρ, surface tension σ and dynamic viscosity η. Densities and surface tensions were measured using a Krüss K12 tensiometer (Krüss, Germany) at room temperature, and the surface tension was obtained using the Wilhelmy plate method, whereas for the density measurements, the tensiometer was equipped with the density setup DE601 (Krüss, Germany). Dynamic viscosities η were measured using a Physica Modular Compact MCR301 rheometer (Anton Paar, Germany) by rotary concentric cylinder rheometry at a temperature of 20 °C and a shear rate of 50 s^{-1}.

Inkjet Printing. Inkjet printing was done by using a piezo-driven drop-on-demand Dimatix-DMP 3000 (Fujifilm, USA) inkjet printer. The printer was equipped with a 16 nozzle printhead (DMC11610, Fujifilm, USA) with a nominal drop volume of 10 pL. To remove any particulate contamination that could interfere with the drop jetting, the inks were filtered through a 0.2 μm syringe filter (PTFE, Chromafil, Machery-Nagel, Germany) and ultrasonicated for 10 min in order to degas. As printing substrates, chemically inert glass slides were used.

■ RESULTS AND DISCUSSION

**Hydrogel Preparation.** Polyelectrolyte hydrogels containing quaternary ammonium groups or sulfonate groups were prepared from aqueous solutions of PEG-DA and one of the ionic monomers, AETA and SPA (Figure 1). For comparison purposes, neutral hydrogels were prepared from aqueous PEG-DA solutions alone. In all cases, curing was achieved photochemically with the aid of the photoinitiator Irgacure 2959. AETA and SPA were chosen because they carry permanent charges and result in polyelectrolyte hydrogels after curing. Thus, ionic interactions with the adsorbates metoprolol (cationic) and diclofenac (anionic) can be expected. Different concentrations of AETA and SPA were aimed at in the fully cured hydrogels in order to gain insight into adsorption mechanisms. UV irradiation of all hydrogel precursor solutions resulted in a transition from a mobile liquid to a soft solid, indicating that curing was successful. In order to assess if in fact the different AETA and SPA concentrations in the hydrogel precursor solutions translated into the cured hydrogels, the gel yields Y and equilibrium degrees of swelling EDS of all hydrogels were measured and are collected in Table 1. Generally, hydrogels without the addition of ionic

Table 1. Hydrogel Characterization Data for the Hydrogels Prepared in This Study[a]

sample	EDS	Y [%]	c_{sulfo} [μmol g^{-1}]	c_{ammon} [μmol g^{-1}]
PEG-DA	4.53 ± 0.02	114 ± 2	0	0
AETA1	5.08 ± 0.10	107 ± 1	0	50.8
AETA3	5.79 ± 0.11	104 ± 3	0	133.8
AETA5	6.13 ± 0.16	107 ± 2	0	210.6
SPA1	4.76 ± 0.06	109 ± 2	45.2	0
SPA3	5.46 ± 0.40	107 ± 13	118.3	0
SPA5	5.58 ± 0.08	114 ± 2	192.9	0

[a]Experimental values are given in mean values ± standard deviation of at least three independent experiments.

monomers exhibited the lowest EDS with a value of 4.53, and with the concentration of ionic monomer in the hydrogel precursor solutions, the EDS of the resulting hydrogels also increased. This effect was more pronounced for AETA-containing hydrogels, for which the highest EDS of 6.13 was achieved for AETA5 hydrogels, whereas SPA5 hydrogels only reached an EDS of 5.58. Calculated gel yields Y were generally all in a similar range for all hydrogels, slightly above 100%, probably because small amounts of residual water, which were very hard to remove in a vacuum, were still present in the hydrogels. The similarity of the Y values indicates that the presence of the ionic monomers did not interfere significantly with hydrogel curing. In addition, the increase in EDS is in accordance with the assumption that a higher concentration of ionic monomers in the hydrogel precursor solutions resulted in a higher concentration of ionic groups incorporated into the hydrogel networks. A similar behavior was described for similar polyelectrolyte hydrogels in the literature before.[27] The data make it reasonable to assume that the polymerizable compounds were converted practically quantitatively during curing. Thus, together with the EDS, it was possible to calculate the concentrations of c_{sulfo} and c_{ammon} of sulfonate and ammonium groups in the hydrogels after swelling (eqs 4 and 5, results see Table 1). Due to the higher EDS of hydrogels with higher concentrations of ionic monomers, the increase of resulting concentrations is less pronounced than the increase of ionic monomer concentrations in the hydrogel precursor solutions. However, c_{ammon} values of 50.8 μmol g^{-1}, 133.8 μmol
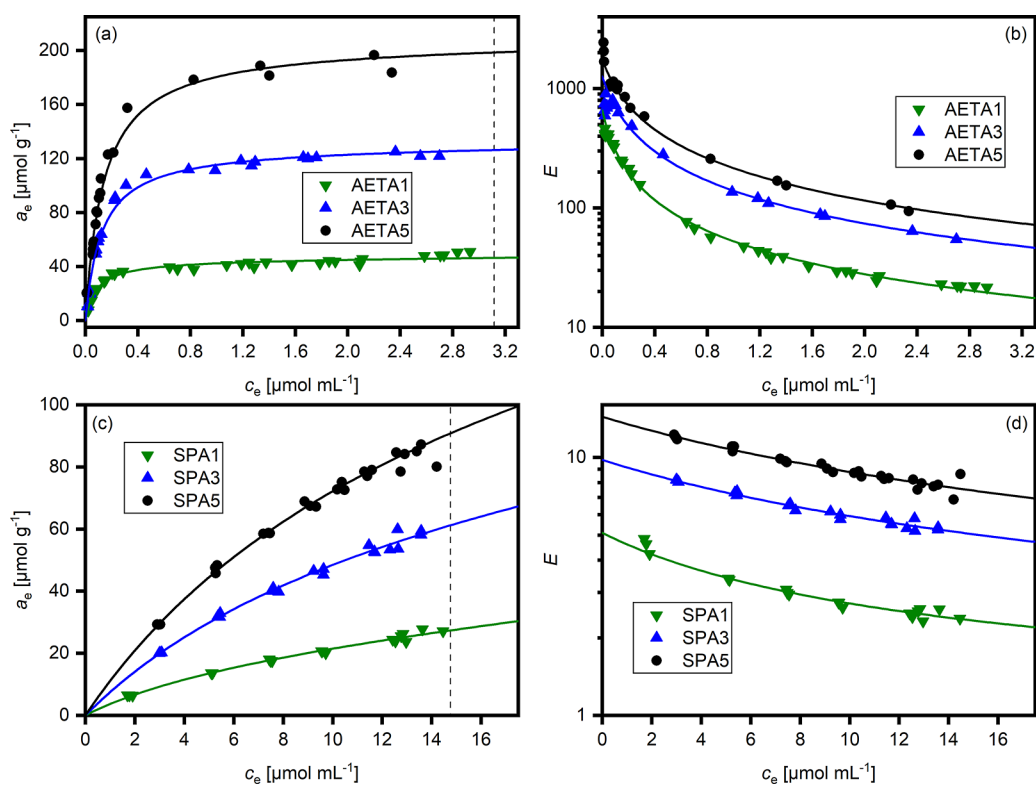
Figure 2. (a) Adsorbate concentrations a_e inside the hydrogels and (b) enhancements factors E against c_e for AETA containing hydrogels with diclofenac as the adsorbate and (c) adsorbate concentrations a_e inside the hydrogels and (d) enhancements factors against c_e for SPA containing hydrogels with metoprolol as the adsorbate. Experimental data points are given by the symbols. The solid lines represent fits according to eqs 10 and 13. The dashed lines give the initial concentration c_0 before adsorption.

g^{-1}, and 210.6 μmol g^{-1} for the AETA hydrogels and c_{sulfo} values of 45.2 μmol g^{-1}, 118.3 μmol g^{-1}, and 192.9 μmol g^{-1} for the SPA hydrogels make the prepared hydrogels suitable for assessing the impact of sulfonate and ammonium groups on the adsorption isotherms with the analytes diclofenac and metoprolol.

HPLC Measurements. For measuring the adsorption isotherms of diclofenac and metoprolol with the hydrogels, hydrogels were immersed into the respective solutions containing the adsorbate molecules. After a defined period of time, the concentration of the adsorbate in the supernatant was determined by HPLC with a diode array detector. Quantification of the adsorbate via HPLC was preferred to simple UV/vis measurements due to the possible formation of soluble hydrolysis products from the hydrogel networks, which could interfere with the measurements. By HPLC, these soluble side products can be separated from the adsorbates, and their concentrations can be measured accurately. HPLC chromatograms of metoprolol and diclofenac obtained with the optimized mobile phase consisting of 80% MES buffer (pH 6.0) and 20% acetonitrile on a C4 stationary phase are shown in the Supporting Information (Figure S1). Under other conditions, such as a C18 stationary phase or using buffers with other pH values (2.1, 4.7, and 8.0), no sufficient retention of metoprolol was observed. The optimized HPLC method applied is generally suitable for the full separation of metoprolol and diclofenac. Also, the peak areas are fully proportional to the concentrations up to at least 1.2 mg mL^{-1}. The corresponding calibrations are shown in the Supporting Information (Figure S2). Generally, the HPLC measurements of solutions after adsorption measurements showed no signs of

hydrogel degradation products, proving the hydrolytic stability of the hydrogels during the experiments.

Adsorption of Charged Adsorbates on Hydrogels with Oppositely Charged Groups. In a first step, the interaction of the ionic compounds diclofenac and metoprolol with hydrogels was assessed using hydrogels with covalently bound ionic groups with opposite charges, i.e., AETA hydrogels for diclofenac and SPA hydrogels for metoprolol. Before measuring adsorption isotherms with these systems, adsorption kinetics were studied. The purpose of these measurements was to make sure the adsorbate was in equilibrium conditions when measuring the equilibrium concentration c_e of the adsorbate in the supernatant after the batch adsorption experiments. Adsorption kinetics were followed with the time-dependent concentrations c_t of the adsorbates in the supernatants. We found that, generally, several hours of adsorption time were necessary to reach a time-independent value of c_e. However, in all cases after 24 h of adsorption time, a constant supernatant concentration was obtained (Figure S3). Therefore, all adsorption experiments were evaluated after 24 h of adsorption time.

Subsequently, the equilibrium concentrations a_e of the adsorbates in the hydrogels were measured and calculated according to eq 6 for different c_e values (Figure 2a,c). It was found that a_e increased with increasing c_e values for both the pairs of AETA hydrogels/diclofenac and SPA hydrogels/ metoprolol. However, the increase in a_e at low c_e was much more pronounced for the AETA hydrogels compared to the SPA hydrogels. After this initial increase, for the AETA hydrogels, a_e values reached a plateau, whereas no plateau was observed for the SPA hydrogels. The differences in the slopes

for the two hydrogel types are also visible when looking at the enhancement factors calculated according to eq 8 (Figure 2b,d). In the AETA hydrogels, enhancement factors reached values up to approximately 1000, whereas for SPA hydrogels enhancement factors were generally not much greater than 10. Thus, diclofenac is enriched in the AETA hydrogels to a much greater extent than metoprolol in the SPA hydrogels. For calculation of the enhancement factors and for all other calculations below, a hydrogel density of 1 g mL^{-1} was assumed due to the high equilibrium water contents.

For a quantitative description of the interaction of adsorbates with hydrogels, the process was divided into two individual steps: In the first step, the adsorbate enters the aqueous phase of the hydrogel and is present in the meshes of the hydrogel network. In the second step, the adsorbate can adsorb onto the polymer network, resulting in an increased residence time of the adsorbate in the hydrogels. Desorption can be regarded as both steps in the opposite direction. This reasoning assumes that the concentrations of the adsorbates in the water phase inside the hydrogels are isotropic. As a physical model for describing the adsorption from the aqueous hydrogel phase, the Langmuir model was used, i.e. the polymer network is assumed to possess a defined number of equal adsorption sites per volume which are fully accessible for all adsorbate molecules. In the Langmuir model, also only one adsorbate molecule can adsorb to one adsorption site, and other interactions do not occur to a significant extent. The adsorption then is equal to an ion exchange with the counterions of the ionic monomers. An isotherm given by pairs of equilibrium adsorbate concentrations a_e and c_e in the hydrogel and the supernatant, respectively, can then be described as a partition isotherm according to eq 10 rather than as an adsorption isotherm only. The main difference of the two approaches is that the Langmuir model tends toward a plateau value q_m at high c_e values, whereas the partition isotherm does not have a plateau value. This is due to the linear term with c_e which could also be considered a dilution term describing the reduction of the initial concentration c_0 by the water contained in the swollen hydrogel.

For Langmuir-type adsorption on hydrogels, eqs 10 and 13 are suitable descriptions. However, other adsorption mechanisms can also play a role and could even be predominant compared to Langmuir adsorption. This was not the case, as shown by experiments with PEG-DA hydrogels prepared under similar conditions without the ionic monomers (Figure S4). PEG-DA hydrogels showed E values of around five for diclofenac and around one for metoprolol. Metoprolol concentrations in PEG-DA hydrogels can therefore be fully explained with partition into the water phase inside the hydrogel; for diclofenac, some weak adsorption occurred. In both cases, E values were much smaller than for the respective AETA and SPA hydrogels (Figure 2), justifying the assumption that in AETA and SPA hydrogels, Langmuir adsorption is predominant and the isotherms assume a Langmuir-type shape. Following this reasoning, the largest effect other than Langmuir adsorption would be expected for AETA1 hydrogels at higher diclofenac concentrations, where the smallest E values are observed (Figure 2a,b, green data points). Indeed, a small deviation of the data points at the highest c_e from the regression line can be seen, which could be caused by non-Langmuir adsorption. However, the effect—if significant at all—is rather small and of little practical relevance because the plateau of the adsorption isotherm would not be used for

sensing applications due to vanishing sensitivity (see discussion below).

Another challenge to be able to use eqs 10 and 13 is knowing the value of $c_{e,H,aq}$, which is not a trivial task to measure directly. It can be expected that $c_{e,H,aq}$ is a function of c_e which can be influenced, e.g., by size exclusion effects or by electrostatic effects such as Donnan exclusion.[20] As a first approximation, we consider the partition of the adsorbates between the supernatant and the water phase inside the hydrogel not to be influenced by such effects, resulting in an ideal partition with $c_{e,H,aq} = c_e$. This approach is also justified by the enhancement factors greater than unity, which shows that exclusion effects are not predominant in these cases. Both for metoprolol and diclofenac, when analyzing the data from Figure 2 under these assumptions, the experimental data can be described very well with eqs 10 and 13 and the Langmuir parameters q_m and K_s are obtained by nonlinear regression (Table 2).

Table 2. Fit Parameters q_m and K_s Resulting from the Nonlinear Regression of Adsorption Isotherms from Figure 2 Using eq 10 ($\pm$ Fit Error)[a]

sample/adsorbate	q_m [μmol g^{-1}]	K_s [mL μmol^{-1}]	ΔG [kJ mol^{-1}]
AETA1/diclofenac	45.0 $\pm$ 0.6	11.70 $\pm$ 0.83	−22.8
AETA3/diclofenac	128.5 $\pm$ 1.8	8.15 $\pm$ 0.49	−21.9
AETA5/diclofenac	204.6 $\pm$ 4.1	7.17 $\pm$ 0.42	−21.6
SPA1/metoprolol	23.3 $\pm$ 1.4	0.14 $\pm$ 0.02	−12.0
SPA3/metoprolol	91.6 $\pm$ 5.8	0.078 $\pm$ 0.009	−10.6
SPA5/metoprolol	153.0 $\pm$ 13.7	0.072 $\pm$ 0.011	−10.4

[a]Values for q_m and K_s are reported referring to diclofenac for the AETA hydrogels and metoprolol for the SPA hydrogels. Values for the free enthalpy of adsorption $\Delta G = -RT \ln(K_s)$ are calculated using K_s divided by L mol^{-1} according to Liu.[28]

Both for AETA and SPA hydrogels, the maximum adsorption capacity q_m obtained from the Langmuir fits of the measured isotherms increased with the concentration of SPA and AETA in the hydrogel precursor solution. This behavior generally is in agreement with the assumption that the ionic groups are the main sites for adsorption on the hydrogels. In order to further quantify the influence of the ionic group concentration in the hydrogels, q_m values were compared to the concentration of ionic groups c_{ammon} and c_{sulfo} in the AETA and SPA hydrogels, respectively (Supporting Information, Figure S5). Under the assumption that each ionic group in a hydrogel can temporarily bind to one oppositely charged adsorbate, q_m should be identical with c_{ammon} and c_{sulfo}, respectively. In fact, a very close correlation between the theoretically expected values and experimentally determined values was observed for the AETA hydrogels. Additionally, the maximum one-to-one interaction of an AETA binding site with a diclofenac molecule, a key assumption of the Langmuir model, seems to be confirmed. Also, other binding events of diclofenac in the AETA hydrogels can be neglected compared with the electrostatic binding of the oppositely charged groups. In contrast, for SPA hydrogels, the q_m values were a little higher than the theoretical values, especially at high SPA concentrations. One explanation could be that the q_e plateau, which should be reached at high c_e values, is not reached in the measurements shown in Figure 2. Thus, the q_m values are obtained by extrapolation. In fact, it was difficult from a practical point of view to reach high q_e values for metoprolol in
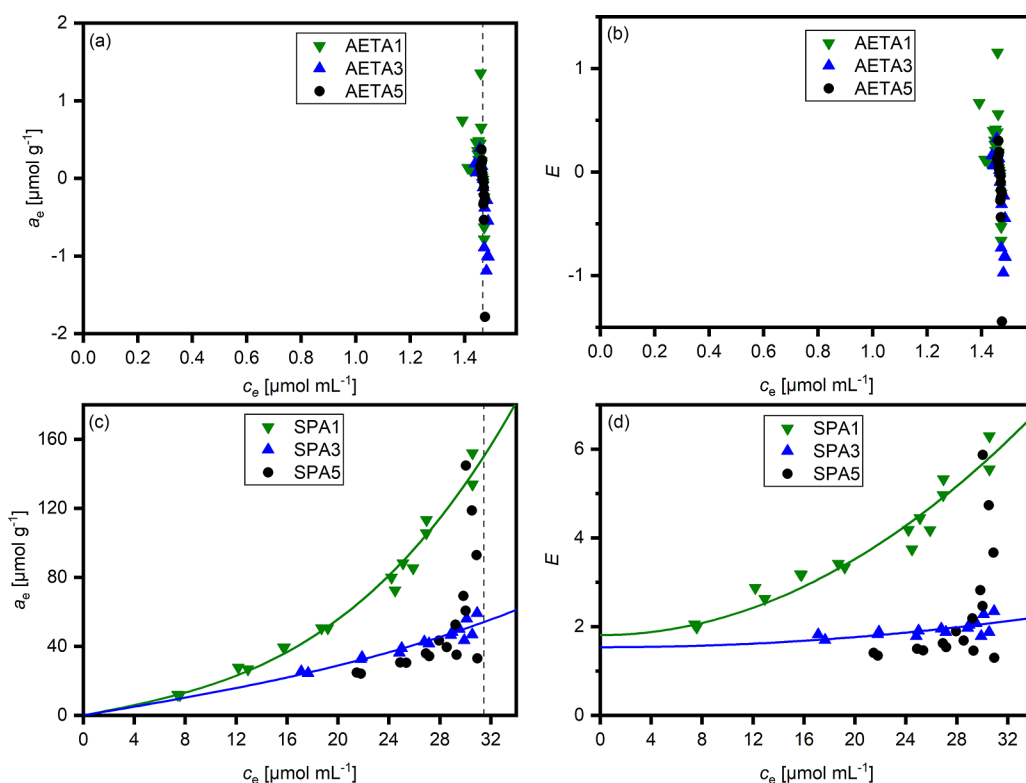
Figure 3. (a) Adsorbate concentrations a_e inside the hydrogels and (b) enhancements factors E against c_e for AETA containing hydrogels with metoprolol as the adsorbate and (c) adsorbate concentrations a_e inside the hydrogels and (d) enhancements factors against c_e for SPA containing hydrogels with diclofenac as the adsorbate. Experimental data points are given by the symbols. The solid lines represent fits according to eqs 11 and 14. The dashed lines give the initial concentration c_0 before adsorption.

SPA hydrogels due to the relatively low enhancement factors. Higher q_e values could either be achieved by using smaller hydrogel masses in the experiments increasing the experimental weighing error or by using higher adsorbate concentrations, which could result in increased interactions between the adsorbate molecules, ultimately reducing their activity coefficient in solution.

The reason for the difference in enhancement factors of metoprolol in SPA hydrogels and diclofenac in AETA hydrogels becomes evident when looking at the K_s values: For diclofenac in AETA hydrogels, the adsorption rate constant on average is 9-fold greater than the desorption rate constant. In contrast, for metoprolol in SPA hydrogels, the desorption rate constant on average is approximately 10-fold greater than the adsorption rate constant. This pronounced difference results in much greater residence times for diclofenac in AETA hydrogels than for metoprolol in SPA hydrogels, leading to the higher E values for diclofenac.

Adsorption of Charged Adsorbates on Hydrogels with Groups of the Same Charge. In comparison with the partition experiments described above, here, adsorbates with the same charge as the ionic groups in the hydrogels were used. More precisely, SPA hydrogels were treated with diclofenac solutions and AETA hydrogels with metoprolol solutions. The resulting data is shown in Figure 3. By looking at the data, it becomes evident directly that partition into the hydrogels is completely different from that above. Looking at the metoprolol partition, both the measured a_e and E values were extremely low and scattered around zero. In fact, in this case, the average value over all E values for metoprolol partition into AETA hydrogels was −0.004, showing that

metoprolol is efficiently excluded from the water phase inside the hydrogels. It is obvious that this behavior is not in accordance with the assumption that $c_{e,H,aq} = c_e$. Therefore, it is not possible to use eqs 10 and 13 to fit the data. No significant difference between the AETA hydrogels was observed. Already with the smallest AETA content, metoprolol cannot enter the hydrogel. Exclusion of metoprolol could be caused by size exclusion or by electrostatic effects such as Donnan exclusion.[29−31] However, we think that size exclusion is unlikely to happen to a significant extent due to the similar molar masses of the diclofenac anion and the metoprolol cation. Additionally, metoprolol was able to enter SPA hydrogels prepared under similar conditions. Also in the case of the PEG-DA hydrogel, molecules with larger molar masses compared to the metoprolol cation, such as adenosine triphosphate (M = 507.18 g mol^{-1}), were shown to be able to diffuse through the polymer network.[7] Therefore, we ascribe the exclusion of metoprolol mainly to Donnan exclusion.

For the SPA hydrogels with diclofenac as the adsorbate, the E values for all c_e values tested were greater than one, indicating that diclofenac was generally able to enter the hydrogels. Interestingly, and in contrast to the partition of metoprolol into SPA hydrogels, E values decreased with increasing SPA concentration. For SPA5 hydrogels, E approached one for the lower c_e values and increased to about six at higher c_e values. The highest E values were observed for the SPA1 hydrogels at high c_e and were in the range of E values observed for the adsorption of diclofenac with PEG-DA hydrogels (Supporting Information, Figure S4). The data suggest that no enrichment of diclofenac in the SPA hydrogels was possible, which exceeded the adsorption in

neutral PEG-DA hydrogels. Further, non-Langmuir adsorption was reduced by higher SPA contents in the hydrogels, up to the point that apparently only partition into the water phase inside the hydrogels occurred for SPA5 hydrogels with $E \approx 1$. Thus, Donnan exclusion was not effective or was dominated by other interactions. In this case, the assumption that $c_{e,H,aq}$ equals c_e might be valid. However, eqs 10 and 13 cannot be applied to fit the data due to the lack of Langmuir-type adsorption, which would result in a decrease of E values with c_e as shown above. Therefore, the data of the SPA1 and SPA3 hydrogels were fitted using an empirical polynomial model according to eqs 11 and 14, resulting in $b_1 = 3.38 \times 10^{-3}$ mL^3 μmol^{-2} g^{-1} and $b_2 = 0.64$ mL g^{-1} (SPA1) and $b_1 = 4.71 \times 10^{-4}$ mL^3 μmol^{-2} g^{-1} and $b_2 = 0.44$ mL g^{-1} (SPA3). The data for SPA5 could not be fitted with either of the two models.

Effect of Adsorption on the Hydrogel Refractive Index. Due to the adsorption of diclofenac on SPA and AETA hydrogels and of metoprolol on SPA hydrogels, it can be expected that their optical properties change and that this change is a function of a_e. Only for the pair of metoprolol and AETA hydrogels, no change in hydrogel properties is expected. In order to use the AETA and SPA hydrogels as adsorbers for optical sensors, the change of optical properties with a_e needs to be known. Therefore, a simple sensor was built, which consisted of a hydrogel disc and a digital refractometer. With this setup and in combination with HPLC, the hydrogel refractive indexes n_D^{20} were measured depending on the concentration a_e of the adsorbates inside the hydrogels (Figure 4). Both for diclofenac adsorption in AETA hydrogels and metoprolol adsorption in SPA hydrogels, a clear linear increase of refractive index with a_e was observed. Also diclofenac adsorption on SPA hydrogels resulted in a slight increase of refractive index, whereas metoprolol did not enter AETA hydrogels, consistent with the observations discussed above (circled data points in Figure 4a). The slopes $\frac{\Delta n_D^{20}}{\Delta a_e}$ of the corresponding linear fits to the data are collected in Table 3.

Refractive index changes with analyte concentration for metoprolol adsorption on SPA hydrogels were in the same order of magnitude as values reported before for metoprolol succinate in aqueous solution at 38 °C (1.21×10^{-4} g μmol^{-1}).[32] We measured a value of 1.13×10^{-4} g μmol^{-1} for metoprolol tartrate at 20 °C. Refractive index changes upon diclofenac adsorption in AETA hydrogels were also similar to our measurements in water at 20 °C (0.70×10^{-4} g μmol^{-1}), although a value as high as 16.1×10^{-4} g μmol^{-1} was reported before.[33] Differences in the refractive index changes might be caused by the presence of the polymer network or by different contributions of adsorbates bound to and not bound by adsorption. For illustration purposes, a concentration of 80 μmol g^{-1} of diclofenac inside a hydrogel corresponds to a mass fraction of 2.5% and of metoprolol to a mass fraction of 5.5%. In can be anticipated that this will have at least a small effect on the EDS. If the EDS was increased, the refractive index will decrease, and such influences could even result in a nearly complete reduction of refractive index change, as seen with diclofenac adsorption on SPA hydrogels. Such behavior can completely rule out the use of an adsorber as a sensor material and should, therefore, be avoided if possible.

Sensor Response and Sensitivity. Taken together, the partition isotherm describing a_e depending on c_e as well as the change of refractive index with a_e will determine the sensor
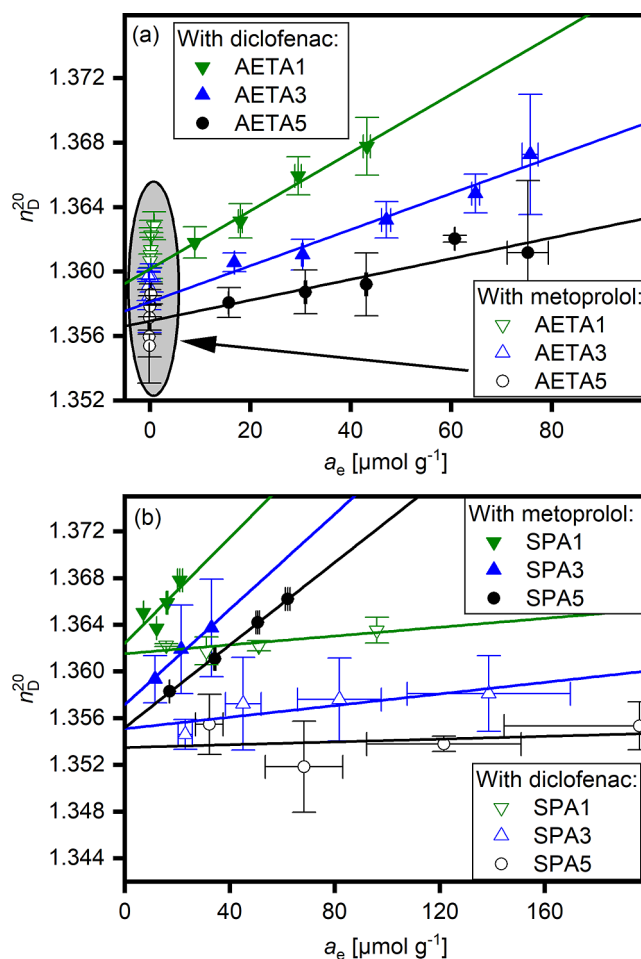
Figure 4. (a) Refractive index n_D^{20} of AETA hydrogels upon adsorption experiments with diclofenac or metoprolol. (b) Refractive index n_D^{20} of SPA hydrogels upon adsorption experiments with diclofenac or metoprolol.

Table 3. Slopes $\frac{\Delta n_D^{20}}{\Delta a_e}$ of the Refractive Index Changes with the Adsorbate Concentration Inside the Hydrogels and the Maximum Sensor Response

	diclofenac		metoprolol	
sample	$\frac{\Delta n_D^{20}}{\Delta a_e}$ [10^{-4} g μmol^{-1}]	$\frac{\Delta n_D^{20}}{\Delta a_e} q_m$	$\frac{\Delta n_D^{20}}{\Delta a_e}$ [10^{-4} g μmol^{-1}]	$\frac{\Delta n_D^{20}}{\Delta a_e} q_m$
AETA1	1.81	0.008	n.a	n.a
AETA3	1.12	0.014	n.a	n.a
AETA5	0.65	0.013	n.a	n.a
SPA1	0.19	n.a	2.26	0.005
SPA3	0.25	n.a	2.04	0.019
SPA5	0.06	n.a	1.77	0.027

response depending on c_e. Thus, the refractive index responses of the hydrogels in this study are given by

$$n_D^{20} = n_D^{20}(0) + \frac{\Delta n_D^{20}}{\Delta a_e} \cdot a_e \tag{15}$$

Here, $n_D^{20}(0)$ is the refractive index of the hydrogel without any adsorbed analyte. The concentration a_e of the analyte inside the hydrogel is a function of the concentration c_e in the surrounding medium. Because in case of enhancement factors

E much greater than one the adsorption on the polymer chains dominates the partition of the adsorbate into the hydrogel water phase, the maximum value of refractive index change can be approximated for Langmuir type adsorption by multiplication of $\frac{\Delta n_D^{20}}{\Delta a_e}$ with q_m (Table 3). Especially for adsorption of diclofenac inside AETA1 hydrogels and of metoprolol in SPA1 hydrogels, the theoretical maximum refractive index change is reached in the experiment (Figure 4) because of saturation of the adsorber. For the other hydrogels, the adsorption capacity is still not exhausted, resulting in refractive index changes smaller than the theoretical maximum.

In order to further asses the sensor response depending on c_e, the sensor sensitivity S, defined as the change of refractive index with c_e,[34] is calculated by the first derivative of eq 15 with c_e

$$S = \frac{dn_D^{20}}{dc_e} = \frac{\Delta n_D^{20}}{\Delta a_e} \cdot \frac{da_e}{dc_e} \tag{16}$$

Using eq 10 for a_e in the case of Langmuir adsorption results in

$$S = \frac{\Delta n_D^{20}}{\Delta a_e} \cdot \left(\frac{\phi_{H_2O}}{\rho_H} + q_m \cdot \frac{K_s}{(c_e \cdot K_s + 1)^2} \right) \tag{17}$$

Similarly, S for the case of hydrogel–adsorbate interaction best described by a polynomial function according to eq 11 results in

$$S = \frac{\Delta n_D^{20}}{\Delta a_e} \cdot \left(\frac{\phi_{H_2O}}{\rho_H} + 3 \cdot b_1 \cdot c_e^2 + b_2 \right) \tag{18}$$

From eqs 17 and 18, the effects the different factors have on S can be deduced for the two cases. As intuitively expected, increasing $\frac{\Delta n_D^{20}}{\Delta a_e}$ results in a linear increase of S in both cases, and it should therefore be maximized. Also, an increased ϕ_{H_2O} can result in an increase of S. However, ϕ_{H_2O} does not result in an enrichment of the adsorbate inside the hydrogel and, if increased, probably results in a decrease of adsorption capacity. Also, the term $\frac{\phi_{H_2O}}{\rho_H}$ will usually be smaller than 1 mL g^{-1} and will therefore be dominated by the adsorption term, making a deliberate maximization of ϕ_{H_2O} less important.

In the Langmuir case (eq 17), an increase in q_m linearly increases S and should therefore be maximized by incorporating as many adsorption sites as possible into the adsorber. K_s is coupled to c_e and therefore their influence on S is less obvious. In order to assess this influence, S is plotted against K_s and c_e according to eq 17 in Figure 5. It becomes apparent that, in all cases, for a given K_s lower c_e values generally result in higher S values, as recognized before.[35] This can be explained by the shape of the Langmuir adsorption isotherm, which gives the highest enrichment factors at the lowest c_e values (see also eq 13 and Figure 2). Therefore, sensors relying on Langmuir adsorption will be most sensitive at low c_e values. As far as K_s for a given c_e is concerned, S does increase only with K_s up to a certain value S_{max} at $K_{s,max}$. In fact, S_{max} is found at the maximum of eq 17 where K_s equals c_e^{-1} (see the red line in Figure 5). Thus, in order to optimize the sensor sensitivity, optimization of K_s is crucial and must be done according to the expected concentrations that the sensor has to measure.
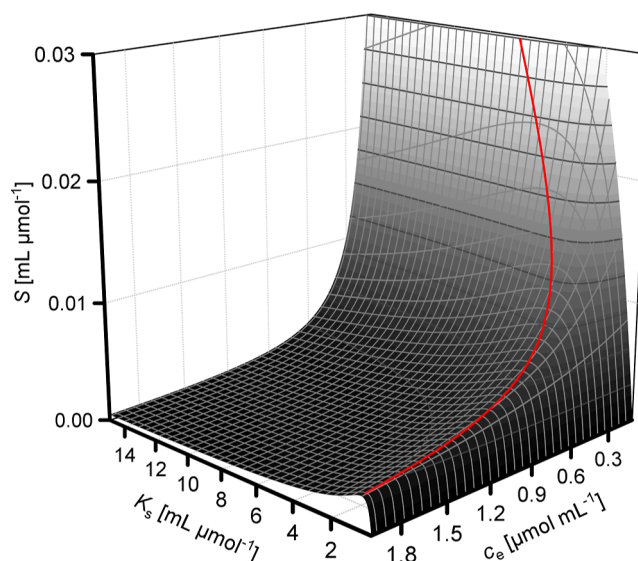

Figure 5. Sensor sensitivity S against K_s and c_e is shown according to eq 17. The red line gives the ideal K_s value as c_e^{-1} for a given c_e. The data was calculated with $\frac{\Delta n_D^{20}}{\Delta a_e} = 0.0002$ g μmol^{-1}, $\frac{\phi_{H_2O}}{\rho_H} = 0.8$ mL g^{-1}, and $q_m = 100$ μmol g^{-1}.

Generally, under ideal conditions, $c_e \ll K_s^{-1}$ should be fulfilled in order to avoid approaching the plateau of the Langmuir adsorption isotherm. If c_e approaches K_s^{-1}, e.g., $c_e = 1$ μmol mL^{-1} and $K_s = 1$ mL μmol^{-1} (Supporting Information, Figure S6), already a substantial loss in sensor sensitivity is present. If $c_e \gg K_s^{-1}$, the sensor sensitivity approaches zero due to the saturation of the Langmuir adsorber. Thus, at rather high c_e values or if a broad concentration range needs to be covered by the sensor, it can be beneficial to use Langmuir adsorbers, which lead to a lower accumulation of the adsorbent in the adsorber by a rather low K_s value. Under such circumstances, although the sensitivities are relatively small, they are still superior to adsorbers with higher K_s values (Supporting Information, Figure S5). Looking at the hydrogels showing Langmuir adsorption behavior, AETA hydrogels should therefore not be used for diclofenac c_e values much above 0.1 μmol mL^{-1}, whereas SPA hydrogels could be used for metoprolol c_e values up to approximately 10 μmol mL^{-1}.

In the case of adsorption described with a polynomial model (eq 17), generally, both b_1 and b_2 should be maximized. An increase in b_2 increases S in a linear way. A larger value of b_1 leads to a bigger curvature of a_e against c_e and therefore to a larger nonlinear increase of S. This type of non-Langmuir adsorption can be optimized by the choice of the material used for the adsorber; however, the general behavior is less predictable than in the Langmuir case.

In the case of sensors relying on refractive index changes, the necessary sensor sensitivity of course is defined by the method of measurement. The refractometer used in this study is able to measure refractive index changes in hydrogels of approximately 10^{-3} and therefore is only good for distinguishing large differences of c_e. More sensitive methods like interferometer-based approaches or SPRS however can be used in future studies in combination with SPA and AETA hydrogels for measuring smaller differences in c_e.

Inkjet Printing. For miniaturization of optical sensors sensitive to refractive index changes, often chips containing
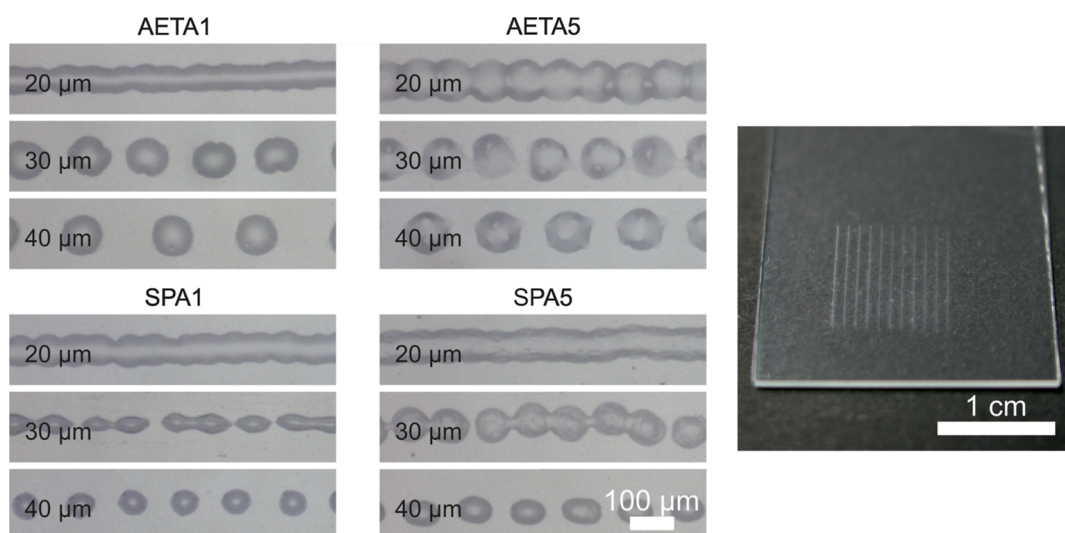
Figure 6. Left and middle columns: Microscopic images of inkjet-printed lines of hydrogel formulations AETA1, AETA5, SPA1, and SPA5 with different drop spacings (20, 30, and 40 μm, as indicated in the figure). The white scale bar in the lower right corner of the SPA5 images is valid for all images. Right: Representative photo of inkjet-printed, cured, and washed AETA5 hydrogel lines, proving successful cross-linking of the printed hydrogel lines.

optical waveguides are used. Light propagation inside the waveguides is then coupled via the evanescent field with the refractive index of the surrounding. In order to accumulate analytes inside the evanescent field, often the waveguide surface is covered with a coating that adsorbs the analyte. Due to the small dimensions of the waveguides in the micrometer range, a coating technique would be desirable, which allowed spatially controlled coating of waveguide containing chips. One technique for this purpose, which was also demonstrated with hydrogel materials,[36] is inkjet printing. Inkjet printing allows to generate more fine structures on surfaces rather than 3D structures, in contrast to extrusion-based 3D printing, which is more often used for hydrogels, including similar formulations to the ones used in the present study.[27] Therefore, our aim was to demonstrate the feasibility of using the described hydrogel formulations for inkjet printing. Another advantage of printing the hydrogel structures is the use of rigid substrates such as glass, which make it possible to use also mechanically weak hydrogels for sensing applications.

However, fluid properties for inkjet printing are quite demanding as low viscosities with suitable surface tensions are required. Therefore, the fluid properties of the inks were measured and are collected in Table S1 (Supporting Information). One dimensionless number that is often used to classify the usability of an ink in piezo-driven Drop-on-Demand (DoD) inkjet printing is Z, the inverse of the Ohnesorge number Oh.

$$Z = \frac{1}{Oh} = \frac{Re}{\sqrt{We}} = \frac{\sqrt{\sigma \rho d}}{\eta} \tag{19}$$

Here, Re is the Reynolds number, and We is the Weber number. Originally introduced by Fromm,[37] Z is often used to measure the applicability of a liquid to be jetted in a DoD printhead. Fromm postulated a value of $Z > 2$ for stable droplet formation. This model was further extended to $1 < Z < 10$ by Reis and Derby.[25] Including more parameters, such as droplet placement precision, Jang et al. concluded a range of $4 < Z < 14$ for stable drop formation.[38] Concerning the different models, the hydrogel ink would fit with Jang et al., whereas

Reis and Derby's model leads to the suggestion that the inks may be troublesome concerning satellite formation. However, during the printing experiments, the droplet formation was stable, and no satellite formation occurred (Supporting Information, Figure S7).

To prove the processability of the hydrogel formulations by inkjet printing, the goal of the inkjet printing experiments was to obtain a continuous line. Therefore, the resolution of the printed pattern was varied by controlling the distance between adjacent droplets, commonly called drop spacing. Figure 6 shows the printed patterns of four different hydrogel formulations (AETA1, AETA5, SPA1, and SPA5) at the three drop spacings of 40, 30, and 20 μm prior to curing. A drop spacing of 40 μm led to separated dots on the substrate. Decreasing the drop spacing to 30 μm brought the droplets closer together. For both the AETA inks, the droplets were still separated, and no line was formed. SPA 1 and SPA 5 showed the first signs of coalescence of the droplets, yet no continuous lines were formed. Therefore, the drop spacing was decreased further to 20 μm. Now, AETA1, SPA1, and SPA5 clearly form a continuous line. Only AETA5 showed liquid beads without fully coalescing into a line. This may be due to differences in the wetting and drying behaviors of the inks. However, in principle, it was shown that the printed hydrogel formulations are capable of being used in an inkjet printing application, and hence, a possible application as coatings for optical waveguides is conceivable. Further optimization of the line formation was not conducted, but line formation and stability of inkjet printer liquids have extensively been discussed elsewhere.[39] Additionally, we studied if the printed lines could be cross-linked under similar conditions to the macroscopic hydrogels above. We generally observed successful curing of all tested formulations, as evidenced by the insolubility of the printed lines after curing (Figure 6 right). We attribute the successful curing to the use of a liquid PEG-DA precursor so that the presumably fast drying of the printed structures did not interfere with the cross-linking.

CONCLUSIONS

Polyelectrolyte hydrogels containing sulfonate groups or quaternary ammonium groups, respectively, were successfully characterized concerning their adsorption with diclofenac and metoprolol. Diclofenac interacts strongly with the hydrogel-bound ammonium groups, resulting in a large enhancement of the diclofenac concentration inside the hydrogels, which can be described with a Langmuir-based partition isotherm. Metoprolol interacts in a similar way with sulfonate groups bound to the hydrogels, although the interaction is much less pronounced. On the other hand, metoprolol was efficiently excluded from hydrogels with ammonium groups, whereas diclofenac was adsorbed weakly on hydrogels with sulfonate groups. Both Langmuir-type adsorption and non-Langmuir adsorption generally were found to lead to well-defined refractive index changes of the hydrogel with the concentration of the adsorbed compound, making them suitable for sensor applications. Additionally, they can be processed by inkjet printing, leading to spatially defined coatings that may be exploited for miniaturized sensors in the future.

It is important to note that the sensors described in this contribution rely on nonspecific and nonselective interactions. It is reasonable to assume that the sensing responses will depend on the presence of other solutes that compete with diclofenac or metoprolol for the adsorption sites. Future work should therefore address this issue by combining the presented hydrogels with other materials and integrating them together into sensor arrays that are able to analyze more complex mixtures of solutes.

ASSOCIATED CONTENT

Supporting Information

The Supporting Information is available free of charge at https://pubs.acs.org/doi/10.1021/acsapm.4c00678.

HPLC calibrations for metoprolol tartrate and diclofenac sodium salt, adsorption kinetics, diclofenac and metoprolol adsorption on PEG-DA hydrogels, sensor sensitivity depending on K_s and c_e in the Langmuir adsorption case, and drop formation during inkjet printing of hydrogel formulations (PDF)

AUTHOR INFORMATION

Corresponding Author

Alexander Southan − Institute of Interfacial Process Engineering and Plasma Technology IGVP, University of Stuttgart, 70569 Stuttgart, Germany; Max Planck Institute for Intelligent Systems, 70569 Stuttgart, Germany; orcid.org/0000-0001-7530-1690; Email: southan@is.mpg.de

Authors

Jennifer Tan − Institute of Interfacial Process Engineering and Plasma Technology IGVP, University of Stuttgart, 70569 Stuttgart, Germany

Fabian Schuster − Institute of Interfacial Process Engineering and Plasma Technology IGVP, University of Stuttgart, 70569 Stuttgart, Germany; Fraunhofer Institute for Interfacial Engineering and Biotechnology IGB, 70569 Stuttgart, Germany

Julia Rotenberger − Institute of Interfacial Process Engineering and Plasma Technology IGVP, University of Stuttgart, 70569 Stuttgart, Germany

Günter E. M. Tovar − Institute of Interfacial Process Engineering and Plasma Technology IGVP, University of Stuttgart, 70569 Stuttgart, Germany; Fraunhofer Institute for Interfacial Engineering and Biotechnology IGB, 70569 Stuttgart, Germany

Complete contact information is available at:
https://pubs.acs.org/10.1021/acsapm.4c00678

Author Contributions

The manuscript was written through the contributions of all authors. All authors have given approval to the final version of the manuscript.

Notes

The authors declare no competing financial interest.

ACKNOWLEDGMENTS

REFERENCES

(1) Laftah, W. A.; Hashim, S.; Ibrahim, A. N. Polymer Hydrogels: A Review. *Polym.-Plast. Technol. Eng.* 2011, *50* (14), 1475−1486.

(2) Claaßen, C.; Southan, A.; Grübel, J.; Tovar, G. E. M.; Borchers, K. Interactions of methacryloylated gelatin and heparin modulate physico-chemical properties of hydrogels and release of vascular endothelial growth factor. *Biomed. Mater.* 2018, *13*, 055008.

(3) Mellott, M. B.; Searcy, K.; Pishko, M. V. Release of protein from highly cross-linked hydrogels of poly(ethylene glycol) diacrylate fabricated by UV polymerization. *Biomaterials* 2001, *22* (9), 929−941.

(4) Yang, J.; Zhang, Y. S.; Yue, K.; Khademhosseini, A. Cell-laden hydrogels for osteochondral and cartilage tissue engineering. *Acta Biomater.* 2017, *57*, 1−25.

(5) Price, C.; Carroll, J.; Clare, T. L. Chemoresistive and photonic hydrogel sensors of transition metal ions via Hofmeister series principles. *Sens. Actuators, B* 2018, *256*, 870−877.

(6) Buenger, D.; Topuz, F.; Groll, J. Hydrogels in sensing applications. *Prog. Polym. Sci.* 2012, *37* (12), 1678−1719.

(7) Majer, G.; Southan, A. Adenosine triphosphate diffusion through poly(ethylene glycol) diacrylate hydrogels can be tuned by cross-link density as measured by PFG-NMR. *J. Chem. Phys.* 2017, *146* (22), 225101.

(8) Caccavo, D.; Cascone, S.; Lamberti, G.; Barba, A. A. Hydrogels: experimental characterization and mathematical modelling of their mechanical and diffusive behaviour. *Chem. Soc. Rev.* 2018, *47* (7), 2357−2373.

(9) Singha, N. R.; Karmakar, M.; Mahapatra, M.; Mondal, H.; Dutta, A.; Roy, C.; Chattopadhyay, P. K. Systematic synthesis of pectin-*g*-(sodium acrylate-co-*N*-isopropylacrylamide) interpenetrating polymer network for superadsorption of dyes/M(II): determination of physicochemical changes in loaded hydrogels. *Polym. Chem.* 2017, *8* (20), 3211−3237.

(10) Fei, Y.; Li, Y.; Han, S.; Ma, J. Adsorptive removal of ciprofloxacin by sodium alginate/graphene oxide composite beads from aqueous solution. *J. Colloid Interface Sci.* 2016, *484*, 196−204.

(11) Zhai, D.; Liu, B.; Shi, Y.; Pan, L.; Wang, Y.; Li, W.; Zhang, R.; Yu, G. Highly Sensitive Glucose Sensor Based on Pt Nanoparticle/Polyaniline Hydrogel Heterostructures. *ACS Nano* 2013, *7* (4), 3540−3546.

(12) Wang, M.; Cui, M.; Liu, W.; Liu, X. Highly dispersed conductive polypyrrole hydrogels as sensitive sensor for simultaneous determination of ascorbic acid, dopamine and uric acid. *J. Electroanal. Chem.* **2019**, *832*, 174−181.

(13) Ehrick, J. D.; Stokes, S.; Bachas-Daunert, S.; Moschou, E. A.; Deo, S. K.; Bachas, L. G.; Daunert, S. Chemically Tunable Lensing of Stimuli-Responsive Hydrogel Microdomes. *Adv. Mater.* **2007**, *19* (22), 4024−4027.

(14) Homola, J.; Yee, S. S.; Gauglitz, G. Surface plasmon resonance sensors: review. *Sens. Actuators, B* **1999**, *54* (1−2), 3−15.

(15) Egger, M.; Tovar, G. E. M.; Hoch, E.; Southan, A. Gelatin methacrylamide as coating material in cell culture. *Biointerphases* **2016**, *11* (2), 021007.

(16) Zhao, Y.; Lei, M.; Liu, S.-X.; Zhao, Q. Smart hydrogel-based optical fiber SPR sensor for pH measurements. *Sens. Actuators, B* **2018**, *261*, 226−232.

(17) Weber, P.; Riegger, B. R.; Niedergall, K.; Tovar, G. E. M.; Bach, M.; Gauglitz, G. Nano-MIP based sensor for penicillin G: Sensitive layer and analytical validation. *Sens. Actuators, B* **2018**, *267*, 26−33.

(18) Fan, X.; White, I. M.; Shopova, S. I.; Zhu, H.; Suter, J. D.; Sun, Y. Sensitive optical biosensors for unlabeled targets: A review. *Anal. Chim. Acta* **2008**, *620* (1−2), 8−26.

(19) Hoppe, N.; Scheck, P.; Sweidan, R.; Diersing, P.; Rathgeber, L.; Vogel, W.; Riegger, B.; Southan, A.; Berroth, M. Silicon Integrated Dual-Mode Interferometer with Differential Outputs. *Biosensors* **2017**, *7* (4), 37.

(20) Dursch, T. J.; Taylor, N. O.; Liu, D. E.; Wu, R. Y.; Prausnitz, J. M.; Radke, C. J. Water-soluble drug partitioning and adsorption in HEMA/MAA hydrogels. *Biomaterials* **2014**, *35* (2), 620−629.

(21) Makhsin, S. R.; Goddard, N. J.; Gupta, R.; Gardner, P.; Scully, P. J. Optimization Synthesis and Biosensing Performance of an Acrylate-Based Hydrogel as an Optical Waveguiding Sensing Film. *Anal. Chem.* **2020**, *92* (22), 14907−14914.

(22) Petrie, B.; Barden, R.; Kasprzyk-Hordern, B. A review on emerging contaminants in wastewaters and the environment: Current knowledge, understudied areas and recommendations for future monitoring. *Water Res.* **2015**, *72*, 3−27.

(23) Kotsmar, C.; Sells, T.; Taylor, N.; Liu, D. E.; Prausnitz, J. M.; Radke, C. J. Aqueous Solute Partitioning and Mesh Size in HEMA/MAA Hydrogels. *Macromolecules* **2012**, *45* (22), 9177−9187.

(24) Gulsen, D.; Chauhan, A. Effect of water content on transparency, swelling, lidocaine diffusion in p-HEMA gels. *J. Membr. Sci.* **2006**, *269* (1−2), 35−48.

(25) Reis, N.; Derby, B. Ink Jet Deposition of Ceramic Suspensions: Modeling and Experiments of Droplet Formation. *MRS Proc.* **2011**, *624*, 65.

(26) Schuster, F.; Hirth, T.; Weber, A. Reactive inkjet printing of polyethylene glycol and isocyanate based inks to create porous polyurethane structures. *J. Appl. Polym. Sci.* **2018**, *136* (3), No. e46977.

(27) Joas, S.; Tovar, G. E. M.; Celik, O.; Bonten, C.; Southan, A. Extrusion-Based 3D Printing of Poly(ethylene glycol) Diacrylate Hydrogels Containing Positively and Negatively Charged Groups. *Gels* **2018**, *4* (3), 69.

(28) Liu, Y. Is the Free Energy Change of Adsorption Correctly Calculated? *J. Chem. Eng. Data* **2009**, *54* (7), 1981−1985.

(29) Manning, G. S. Limiting Laws and Counterion Condensation in Polyelectrolyte Solutions I. Colligative Properties. *J. Chem. Phys.* **1969**, *51* (3), 924−933.

(30) Geise, G. M.; Paul, D. R.; Freeman, B. D. Fundamental water and salt transport properties of polymeric materials. *Prog. Polym. Sci.* **2014**, *39* (1), 1−42.

(31) Ilyas, S.; Abtahi, S. M.; Akkilic, N.; Roesink, H. D. W.; de Vos, W. M. Weak polyelectrolyte multilayers as tunable separation layers for micro-pollutant removal by hollow fiber nanofiltration membranes. *J. Membr. Sci.* **2017**, *537*, 220−228.

(32) Deosarkar, S. D.; Kalyankar, T. M. Structural properties of aqueous metoprolol succinate solutions. Density, viscosity, and refractive index at 311 K. *Russ. J. Phys. Chem. A* **2013**, *87* (6), 1060−1062.

(33) Iqbal, M. J.; Chaudhry, M. A. Thermodynamic study of three pharmacologically significant drugs: Density, viscosity, and refractive index measurements at different temperatures. *J. Chem. Thermodyn.* **2009**, *41* (2), 221−226.

(34) Fraden, J. *Handbook of Modern Sensors: Physics, Designs, and Applications*; Springer, 2016.

(35) Paolesse, R.; Nardis, S.; Monti, D.; Stefanelli, M.; Di Natale, C. Porphyrinoids for Chemical Sensor Applications. *Chem. Rev.* **2017**, *117* (4), 2517−2583.

(36) Southan, A.; Hoch, E.; Schönhaar, V.; Borchers, K.; Schuh, C.; Müller, M.; Bach, M.; Tovar, G. E. M. Side Chain Thiol-functionalized Poly(ethylene glycol) by Post-polymerization Modification of Hydroxyl Groups: Synthesis, Crosslinking and Inkjet Printing. *Polym. Chem.* **2014**, *5* (18), 5350−5359.

(37) Fromm, J. E. Numerical Calculation of the Fluid Dynamics of Drop-on-Demand Jets. *IBM J. Res. Dev.* **1984**, *28* (3), 322−333.

(38) Jang, D.; Kim, D.; Moon, J. Influence of Fluid Physical Properties on Ink-Jet Printability. *Langmuir* **2009**, *25* (5), 2629−2635.

(39) Stringer, J.; Derby, B. Limits to feature size and resolution in ink jet printing. *J. Eur. Ceram. Soc.* **2009**, *29* (5), 913−918.